

## Cation distribution study of $\text{Nd}^{3+}$ substituted Zn-Mg spinel ferrites by structural refinement method

B P Ladgaonkar, P N Vasambekar and A S Vaingankar\*

Department of Electronics, Shivaji University,  
Kolhapur-416 004, Maharashtra, India

E-mail : anil\_vaingankar@yahoo.com

**Abstract** : Assuming preferential distribution of magnesium ion among tetrahedral (A) and octahedral (B) site the cation distribution is predicted for  $\text{Nd}^{3+}$  substituted Zn-Mg ferrites. Cation distribution is investigated by a method wherein structural refinement is applied. The theoretical intensity of X-ray reflections, which found to depend on site occupancy, was calculated. The dependence of intensity of reflections against cation distribution parameter was studied which suggests that the intensity of (220) and (422) reflections are sensitive to A-site, whereas that of (222) and (400) to the B-site. Close agreement of the theoretically calculated and experimentally observed intensity supports the predicted cation distribution. To counter check, the simplified method wherein graph of theoretical intensity of (220) reflections is plotted against distribution parameter. By plotting observed intensity of the same plane the exact distribution parameter is decided with the help of this plot. The plot of reliability factor, R against distribution parameter shows deep near about exact distribution parameter, which supports the exactness of cation distribution. The investigated cation distribution reveals that zinc ion shows its strong occupancy on A-site and magnesium ion distributes partially among A and B sites indicating maximum occupancy on A site for  $x = 0.20$ . The substituted  $\text{Nd}^{3+}$  ion resides on B-site displacing proportional amount of magnesium from B site to A site.

**Key words** : Polycrystalline ferrite, cation distribution, X-ray intensity

**PACS Nos.** 75.50 Gg, 61.10.Nz, 61.66.-f

### 1. Introduction

Spinel ferrites have two magnetic sublattices, tetrahedral A-site and octahedral B-site. The structural, electrical and magnetic properties, upon which its application depends, are found to be sensitive to distribution of cations among these sites [1]. In order to interpret the results regarding these intrinsic properties, the knowledge of cation distribution turns out to be essential. Therefore, investigation of cation distribution in ferrites system is of interest. The cation distribution can be investigated by the Gell'io statistical model in which three magnetic ions per formula unit is considered [2]. However, the present system does not consist three magnetic ions per formula units. Upadhyay and Balda [3] have suggested the method to estimate cation distribution, assuming relative weighted magnetic interaction per formula unit. This was further modified by Vasambekar *et al* [4] for trivalent substitution.

By process of structural refinement of X-ray powder diffractograms, much structural information can be obtained [5,6]. The intensity of X-ray reflections provides the information

regarding occupancy of cations among these sites [1, 7], whereas full width at half maximum (FWHM) gives particle size [5]. The intensity of 220 and 422 reflections strongly depends on cations of tetrahedral site [7], while that of 222 and 400 is sensitive to cations of octahedral site [8]. Assuming this dependence, the structural refinement method is used and the results regarding the study of cation distribution investigation by structural refinement for  $\text{Nd}^{3+}$  substituted Zn-Mg ferrites are reported.

### 2. Experimental

Compositions of polycrystalline ferrites,  $\text{Zn}_x\text{Mg}_{1-x}\text{Fe}_{2-y}\text{Nd}_y\text{O}_4$  ( $x = 0.00, 0.20, 0.40, 0.60, 0.80$  and  $1.00$ ;  $y = 0.00$  and  $0.05$ ) were prepared by standard ceramic method, wherein the AR grade oxides  $\text{ZnO}$ ,  $\text{MgO}$ ,  $\text{Fe}_2\text{O}_3$  and  $\text{Nd}_2\text{O}_3$  were employed. The sintering temperature was controlled at  $1000^\circ\text{C}$  for 24 hours and the furnace was slowly cooled. To confirm the completion of solid state reaction, the compositions were characterized by standard tools *i.e.* X-ray, FIR absorption and SEM. The diffractograms were further subjected for structural refinement to investigate the cation distribution.

\* Corresponding Author

### 3. Results and discussion

The X-ray diffractograms of powdered compositions reveal the formation of single phase cubic spinels, showing well defined reflections of allowed planes. On refinement of the diffractograms, the extracted structural data are presented in Table 1. The lattice constant, as indicated in Table 1, exhibits linear relationship with  $Zn^{2+}$  concentration obeying Vegard's law. This may be due to large ionic radius of  $Zn^{2+}$  ion ( $r_{Zn^{2+}} = 0.83 \text{ \AA}$ ), which when substituted resides on tetrahedral A-site and displaces smaller  $Fe^{3+}$  ion ( $r_{Fe^{3+}} = 0.67 \text{ \AA}$ ) from A site to B site. This suggests the strong occupancy of  $Zn^{2+}$  ion on tetrahedral A-site [9]. Due to  $Nd^{3+}$  substitution the lattice constant is found to be decreasing slightly. Such reduction in the lattice constant in rare-earth

substituted ferrites system was reported by Rezlescu and Rezlescu [10], suggesting the occupancy of rare-earth ion on B-site.

The physical densities ( $dp$ ) of the compositions were measured by using liquid method and are reported in Table 1 along with X-ray density ( $dx$ ) and porosity ( $P$ ). The cation-oxygen bond lengths for tetrahedral A-site, ( $A-O$ ) and for octahedral B-site ( $B-O$ ) were calculated by using relations  $A-O = (u-1/8)a\sqrt{3}$  and  $B-O = (5/8-U)a$  and are presented in Table 1. The  $A-O$  bond length shows increasing trend with  $Zn^{2+}$  concentration, while B-O bond length decreases with increasing  $Zn^{2+}$  ion. This can be attributed to the strong occupancy of  $Zn^{2+}$  ion on A-site. Tetrahedral site ( $R_A$ ) and

Table 1. Structural data for the compositions of  $Zn_xMg_{1-x}Fe_yNd_yO_4$  ferrites system.

Compositions $\Rightarrow$	x	0 00	0 20	0.40	0 60	0.80	1.00
Parameters $\Downarrow$		y = 0.00					
Lattice constants, (a) $\text{\AA}$		8.33	8.53	8.37	8.39	8.41	8.43
No. of Formula unit, (Z)		8	8	8	8	8	8
Formula weight, (w) gm.		200.02	208.23	216.44	224.65	232.8	241.08
X-ray Density, (dx) $\text{gm/cm}^3$		3.99	4.01	4.22	4.54	4.64	4.81
Physical Density, (dp) $\text{gm/cm}^3$		4.64	4.79	4.95	5.10	5.27	5.40
Porosity (P) %		13.89	16.36	14.44	10.39	11.98	11.00
Bond distance, (A-O) $\text{\AA}$		1.72	1.78	1.82	1.86	1.87	1.94
Bond distance, (B-O) $\text{\AA}$		2.13	2.11	2.09	2.08	2.08	2.04
Tetrahedral Radius, ( $R_A$ ) $\text{\AA}$		0.37	0.43	0.47	0.51	0.52	0.59
Octahedral Radius, ( $R_B$ ) $\text{\AA}$		0.783	0.755	0.739	0.727	0.725	0.691
R-Factors	$R_B$	0.0045	0.0197	0.0108	0.0065	0.0069	0.0183
	$R_p$	0.0051	0.0233	0.0127	0.0066	0.0068	0.0178
	$R_{wp}$	0.017	0.042	0.023	0.012	0.018	0.035
	S	0.056	0.123	0.125	0.064	0.097	0.190
Oxygen ion parameter (U) $\text{\AA}$		0.369	0.373	0.355	0.377	0.378	0.383
		y=0.05					
Lattice constants, (a) $\text{\AA}$		8.31	8.33	8.35	8.37	8.39	8.41
No. of Formula unit, (Z)		8	8	8	8	8	8
Formula weight, (w) gm.		204.23	212.44	220.66	228.87	237.08	245.29
X-ray Density, (dx) $\text{gm/cm}^3$		4.13	4.15	4.39	4.45	4.50	4.79
Physical Density, (dp) $\text{gm/cm}^3$		4.65	4.82	4.99	5.16	5.33	5.49
Porosity, (P) %		11.26	13.75	11.86	13.67	15.48	12.57
Bond distance, (A-O) $\text{\AA}$		1.71	1.78	1.81	1.85	1.87	1.92
Bond distance, (B-O) $\text{\AA}$		2.13	2.10	2.08	2.07	2.07	2.05
Tetrahedral Radius, ( $R_A$ ) $\text{\AA}$		0.36	0.43	0.46	0.50	0.52	0.57
Octahedral Radius, ( $R_B$ ) $\text{\AA}$		0.782	0.751	0.736	0.727	0.719	0.695
R-Factors	$R_B$	0.0228	0.0201	0.0174	0.0092	0.0260	0.0319
	$R_p$	0.0212	0.0209	0.0116	0.0103	0.0248	0.0304
	$R_{wp}$	0.057	0.044	0.050	0.026	0.056	0.069
	S	0.305	0.231	0.266	0.142	0.299	0.370
Oxygen ion parameter, (U) $\text{\AA}$		0.368	0.373	0.375	0.377	0.378	0.382

octahedral site ( $R_B$ ) radii have been calculated by using relation from Smith and Wijn [11],  $R_A = (u - 1/4)a\sqrt{3} - R_0$  and  $R_B = (5/8 - u)a - R_0$ , where  $R_0$  is the radius of oxygen and  $u$  is the oxygen ion parameter. On close inspection of Table 1, it is found that the tetrahedral radius increases with increasing  $\text{Zn}^{2+}$  concentration, whereas that of octahedral site decreases. This also supports the occupancy of  $\text{Zn}^{2+}$  ion on A-site.

X-ray powder diffractograms consists much structural information, which can be explored by structural refinement [5, 6]. According to Rietveld [5], the intensity of reflection observed at Bragg's position  $\theta_k$  is given by

$$I_k = |F_k|^2 P_k L_k \left\{ C_0^{1/2} / H_k \sqrt{\pi} \right\} \exp \left[ -C_0 (2\theta_k)^2 / H_k^2 \right], \quad (1)$$

where  $|F_k|^2$  is the total structure factor, obtained by summing the atomic scattering factors of all 56 atoms along with their positional co-ordinates. Since the cubic spinel has space group  $\text{Fd}\bar{3}m$  [7], the positional co-ordinates used are  $8a$  and  $16c$  for cations of tetrahedral and octahedral site respectively and  $32e$  for oxygen ion [1]. The atomic scattering factors were obtained from eq. (15)

$$f(s) = \sum a_i \exp(-b_i s^2) + c_i, \quad (2)$$

where  $a_i$ ,  $b_i$  and  $c_i$  are the coefficient obtained from least curve fitting.  $P_k$  is the multiplicity of the reflections and  $L_k$  is Lorentz polarization factor. Since the Gaussian distribution function was considered as profile function, the constant  $C_0$  could be equal to  $4\log 2$  [12]. The term  $H_k$  is Full Width at Half Maximum (FWHM), takes account of peak broadening resulting from particle size and is given by  $H_k^2 = u \tan^2 \theta + v \tan \theta + w$ , where  $u$ ,  $v$  and  $w$  are the half width parameters. The reliability of structural refinement is usually expressed in terms of reliability factors  $R_B$ ,  $R_p$ ,  $R_{wp}$  and  $S$ , the goodness of fit [13,14]. These factors have been calculated and presented in Table 1. The values of the parameters are found to be less than 0.15, the limit of reliability [15, 16], which supports the refinement.

Assuming preferential occupancy of  $\text{Mg}^{2+}$  ion on either sites, the formula proposed for cation distribution is

$$(\text{Zn}_x \text{Mg}_\delta \text{Fe}_{1-x-\delta})^A [\text{Mg}_{1-x-\delta} \text{Fe}_{1+x+\delta-y}]^B \text{O}_4, \quad (3)$$

where  $\delta$  is the distribution parameter, which gives amount of  $\text{Mg}^{2+}$  ion occupying tetrahedral A- site. By using eq. (1), the theoretical intensities of reflections were calculated and the ratio  $I/I_{\text{max}}$  is used for interpretation of the results. In order to confirm the dependence of intensity of reflections on site occupancy, the intensities of various reflections have been calculated as a function of distribution parameter  $\delta$  in the range from 0 to  $1-x$  and plotted against distribution parameter  $\delta$ , as depicted in Figure 1. On inspection of Figure 1, it is observed that intensity of 220 and 422 reflection decreases with increasing  $\delta$ , whereas

the intensity of 222 and 400 reflections increases with increasing  $\delta$ . This may be attributed to the sensitivity of 220 and 422 reflection to the cations of tetrahedral A-site and that of 222 and

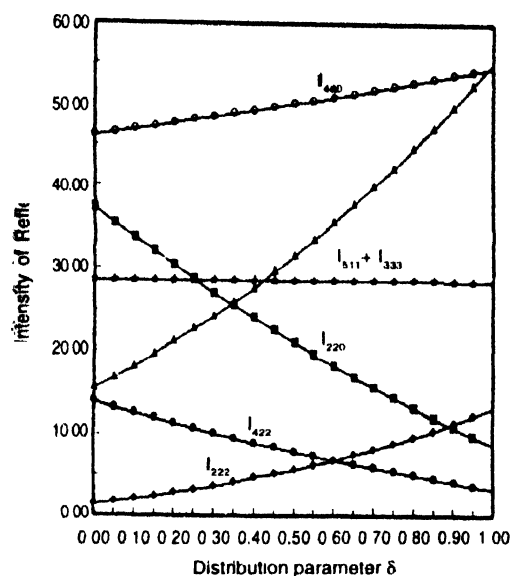


Figure 1 Theoretical intensity of reflection vs distribution parameters  $\delta$

400 reflections to the cations of octahedral B-site. If amount of lighter  $\text{Mg}^{2+}$  ion ( $\delta$ ) increases, then equal amount of heavier  $\text{Fe}^{3+}$  ion shifts from A-site to B-site. This results into decrease in the total structure factor ( $F_A$ ) of A-site and increase in total structure ( $F_B$ ) of B-site. The clubed intensity  $I_{511} + I_{333}$ , remains independent on  $\delta$ ; however, it shows increasing trend with oxygen ion parameter ( $u$ ), as shown in Figure 2. The oxygen ion parameter was decided by placing observed intensity of  $I_{511} + I_{333}$  on this plot. Thus obtained  $u$ -parameters are reported in Table 1.

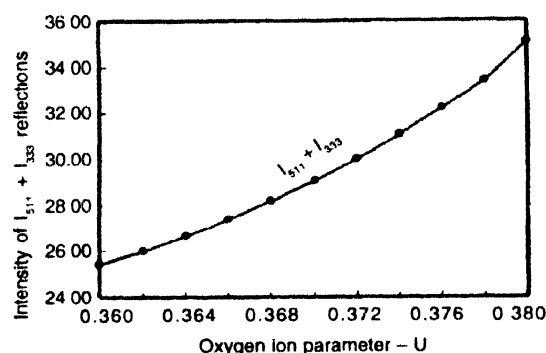


Figure 2. Intensity of  $I_{511} + I_{333}$  reflection vs oxygen ion U-parameter

The intensity of 220 reflection being sensitive to A-site, is calculated as a function for distribution parameter  $\delta$  and plotted versus  $\delta$ . The expanded part of this plot is shown in Figure 3, typically for  $x = 0.40$ ;  $y = 0.00$  and  $0.05$ . The exact value of distribution parameter  $\delta$  is obtained by placing observed intensity of 220 reflection on the same plot, as indicated in the Figure 3. These values of exact distribution parameter  $\delta$  are

used to predict cation distribution. The refinement factors  $R_B$  were also calculated as a function of  $\delta$  and plotted against  $\delta$  as depicted in Figure 3. By inspection of Figure 3, it is found that the refinement factor shows the dip near about exact value of  $\delta$ .

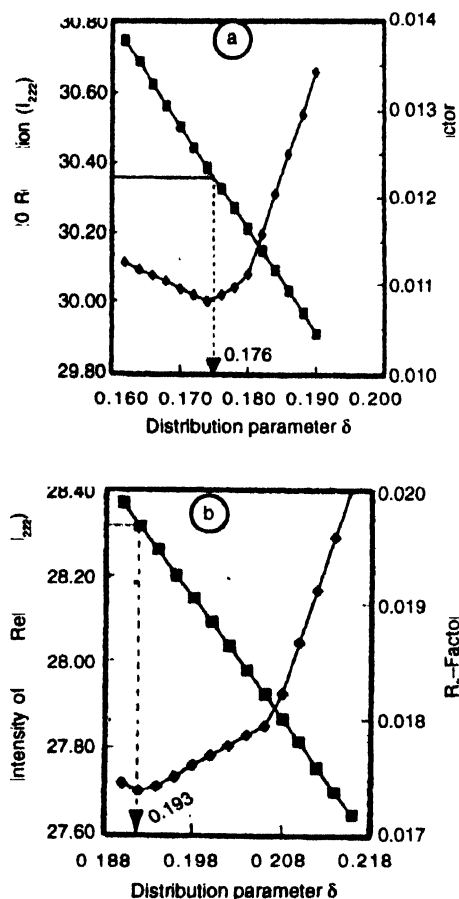


Figure 3. Theoretical intensity of 220 reflection and reliability index  $R_B$  vs distribution parameter  $\delta$ . (a)  $x = 0.40$  ;  $y = 0.00$  and (b)  $x = 0.40$  ;  $y = 0.05$ .

This dip in the refinement factor supports the exactness of the distribution parameter  $\delta$  and hence proposed cation distribution. The investigated cation distribution is presented in Table 2. The cation distribution presented in Table 2 shows good agreement with the previous reports for  $\text{MgFe}_2\text{O}_4$  ferrite [17]. The occupancy of magnesium ion on tetrahedral site increases with  $\text{Zn}^{2+}$  concentration ( $x$ ) up to  $x = 0.20$  and decrease thereafter. On  $\text{Nd}^{3+}$  substitution, the amount of  $\text{Mg}^{2+}$  ion occupying A site increases. This also supports the occupancy on  $\text{Nd}^{3+}$  ion on B site.

#### 4. Conclusion

Structural refinement method can be used to estimate the exact cation distribution. The intensity of reflection shows its dependence on site occupancy and oxygen ion parameter. The exact distribution parameter can be decided by comparing observed intensity with calculated one. The refinement factor shows a deep near about the exact distribution parameters, which support the exactness of the method. The cation distribution investigation shows that the occupancy of magnesium ion on tetrahedral site increases up to  $x = 0.2$  and decreases thereafter. The substituted  $\text{Nd}^{3+}$  ion resides on B-site and results into increase of magnesium ion on A-site.

#### References

- [1] B P Ladgaonkar and A S Vaingankar *Mater. Chem. Phys.* **56/3** 280 (1998)
- [2] M A Gelli'o *J. Phys. Chem. Sol.* **13** 33 (1960)
- [3] R V Upadhyay and G L Balda *Indian J. Phys.* **A63** 835 (1989)
- [4] P N Vasambekar, C B Kolekar and A S Vaingankar *J. Magn. Mater.* **186** 333 (1998)
- [5] H M Rietveld *J. Appl. Cryst.* **2** 65 (1969)
- [6] H M Rietveld *Acta Cryst.* **22** 151 (1967)

Table 2. Cation distribution for the compositions of  $\text{Zn}_x\text{Mg}_{1-x}\text{Fe}_2\text{Nd}_y\text{O}_4$  ferrites system

$\text{Zn}^{2+}$ conc. $x$	$\text{Nd}^{3+}$ conc. $y$	Cation distribution	Distribution parameter $\delta$
0.0	0.00	$(\text{Zn}_{0.00}\text{Mg}_{0.124}\text{Fe}_{0.876})^A(\text{Mg}_{0.876}\text{Fe}_{1.124}\text{Nd}_{0.00})^B\text{O}_4$	0.124
0.2		$(\text{Zn}_{0.20}\text{Mg}_{0.186}\text{Fe}_{0.814})^A(\text{Mg}_{0.814}\text{Fe}_{1.186}\text{Nd}_{0.00})^B\text{O}_4$	0.186
0.4		$(\text{Zn}_{0.40}\text{Mg}_{0.176}\text{Fe}_{0.824})^A(\text{Mg}_{0.824}\text{Fe}_{1.176}\text{Nd}_{0.00})^B\text{O}_4$	0.176
0.6		$(\text{Zn}_{0.60}\text{Mg}_{0.063}\text{Fe}_{0.937})^A(\text{Mg}_{0.937}\text{Fe}_{1.063}\text{Nd}_{0.00})^B\text{O}_4$	0.063
0.8		$(\text{Zn}_{0.80}\text{Mg}_{0.009}\text{Fe}_{0.991})^A(\text{Mg}_{0.991}\text{Fe}_{1.009}\text{Nd}_{0.00})^B\text{O}_4$	0.009
1.0		$(\text{Zn}_{1.00}\text{Mg}_{0.000}\text{Fe}_{0.999})^A(\text{Mg}_{0.000}\text{Fe}_{2.000}\text{Nd}_{0.00})^B\text{O}_4$	0.000
0.0	0.05	$(\text{Zn}_{0.00}\text{Mg}_{0.125}\text{Fe}_{0.875})^A(\text{Mg}_{0.875}\text{Fe}_{1.075}\text{Nd}_{0.05})^B\text{O}_4$	0.125
0.2		$(\text{Zn}_{0.20}\text{Mg}_{0.198}\text{Fe}_{0.802})^A(\text{Mg}_{0.802}\text{Fe}_{1.198}\text{Nd}_{0.05})^B\text{O}_4$	0.198
0.4		$(\text{Zn}_{0.40}\text{Mg}_{0.191}\text{Fe}_{0.807})^A(\text{Mg}_{0.807}\text{Fe}_{1.191}\text{Nd}_{0.05})^B\text{O}_4$	0.193
0.6		$(\text{Zn}_{0.60}\text{Mg}_{0.086}\text{Fe}_{0.914})^A(\text{Mg}_{0.914}\text{Fe}_{1.086}\text{Nd}_{0.05})^B\text{O}_4$	0.086
0.8		$(\text{Zn}_{0.80}\text{Mg}_{0.024}\text{Fe}_{0.976})^A(\text{Mg}_{0.976}\text{Fe}_{1.024}\text{Nd}_{0.05})^B\text{O}_4$	0.024
1.0		$(\text{Zn}_{1.00}\text{Mg}_{0.000}\text{Fe}_{0.999})^A(\text{Mg}_{0.000}\text{Fe}_{1.999}\text{Nd}_{0.01})^B\text{O}_4$	0.000

- [7] E Wolska, E Riedel and W Wolski *Phys. Stat. Soli. A* **132** K51 (1992)
- [8] L Cervinka and Z Simsa *Czech J Phys* **B20** 470 (1990)
- [9] B P Ladgaonkar, C B Kolekar and A S Vaingankar *Bull. Mater. Sci.* **22** 5 917 (1999)
- [10] N Rezlescu and E Rezlescu *Proc. ICF* **7** 225 (1997)
- [11] J Smith and H P J Wijn *Ferrites* (Philips Tech. Library, Eindhoven, The Netherlands) (1959)
- [12] D B Wiles and R A Young *J. Appl. Cryst* **14** 149 (1987)
- [13] R A Young, P E Mackie and R B Von Dreele *J Appl Cryst* **10** 262 (1977)
- [14] G Malmros and John O Thomas *J Appl Cryst* **10** 7 (1977)
- [15] H Lipson and W Cochran *Determination of Crystal Structure Vol. III* (London Bell) 140 (1970)
- [16] *International Table for X-ray Crystallography Vol. I* (Birmingham Kynoch) (1969)
- [17] B R Karche, B V Khasbardar and A S Vaingankar *J Magn Magn Mater* **168** 292 (1997)